

**Supporting Information:**

**Electroactivation-induced IrNi Nanoparticles at Different pH  
Conditions for Neutral Water Oxidation**

**Woong Hee Lee <sup>a†</sup>, Jaekyung Yi <sup>a, b†</sup>, Hong Nhan Nong <sup>c</sup>, Peter Strasser <sup>c</sup>, Keun Hwa Chae <sup>d</sup>, Byoung Koun Min <sup>a, e</sup>, Yun Jeong Hwang <sup>a, b, f\*</sup>, and Hyung-Suk Oh <sup>a, b \*</sup>**

<sup>a</sup> *Clean Energy Research Center, Korea Institute of Science and Technology (KIST), Hwarang-ro 14-gil 5, Seongbuk-gu, Seoul 02792, Republic of Korea*

<sup>b</sup> *Division of Energy and Environmental Technology, KIST school, Korea University of Science and Technology, Seoul 02792, Republic of Korea*

<sup>c</sup> *The Electrochemical Energy, Catalysis, and Materials Science Laboratory, Department of Chemistry, Chemical Engineering Division, Technical University Berlin, Berlin 10623, Germany*

<sup>d</sup> *Advanced Analysis Center, Korea Institute of Science and Technology (KIST), Hwarang-ro 14-gil 5, Seongbuk-gu, Seoul 02792, Republic of Korea*

<sup>e</sup> *Green School, Korea University, 145 Anam-ro, Seongbuk-gu, Seoul 02841, Republic of Korea*

<sup>f</sup> *Department of Chemical and Biomolecular Engineering, Yonsei-KIST Convergence Research Institute, Yonsei University, Seoul 03722, Republic of Korea*

† The authors have contributed equally to this work.

\*Corresponding author  
Email: yjhwang@kist.re.kr, hyng-suk.oh@kist.re.kr  
Tel: +82 (0)2 952 5292

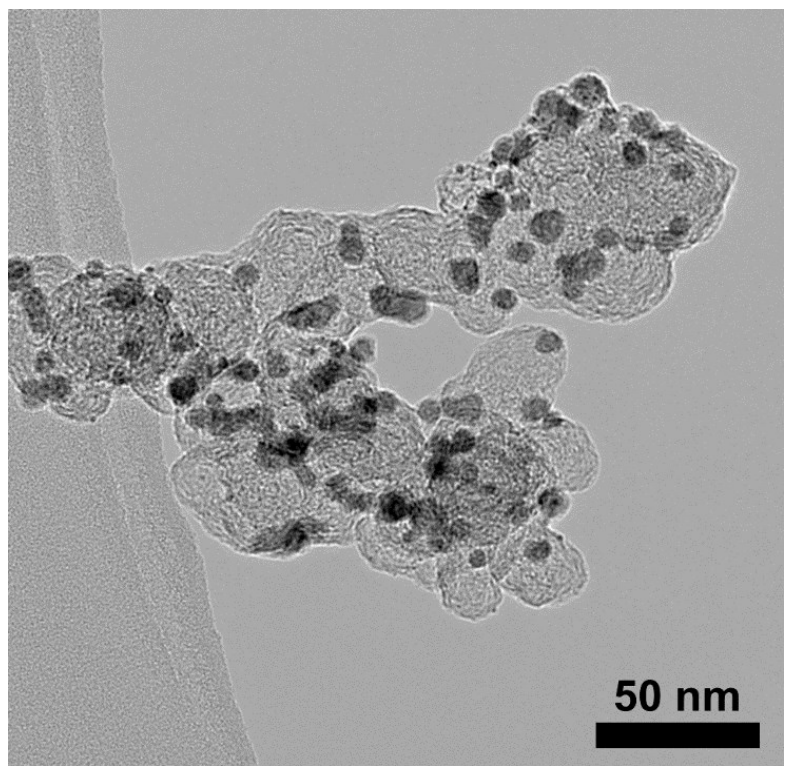


**Figure S1.** HR-TEM images of the pristine IrNi nanoparticles supported on carbon black (IrNi/C)

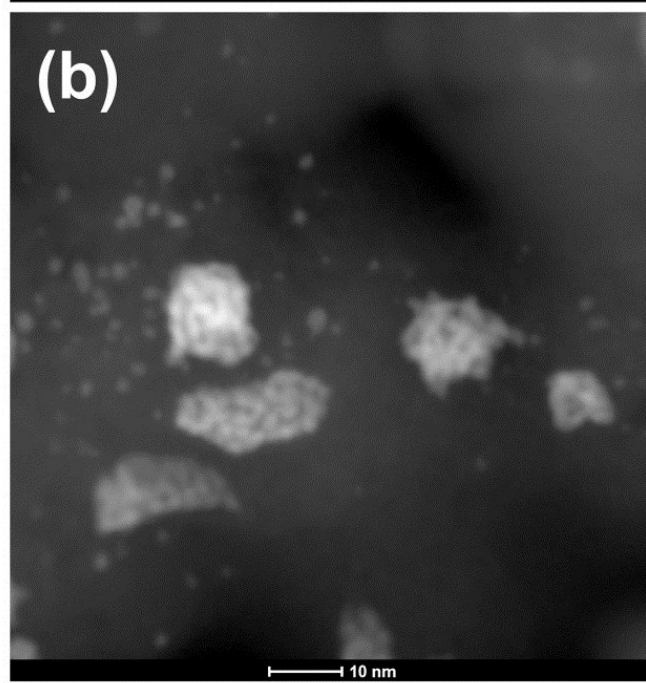
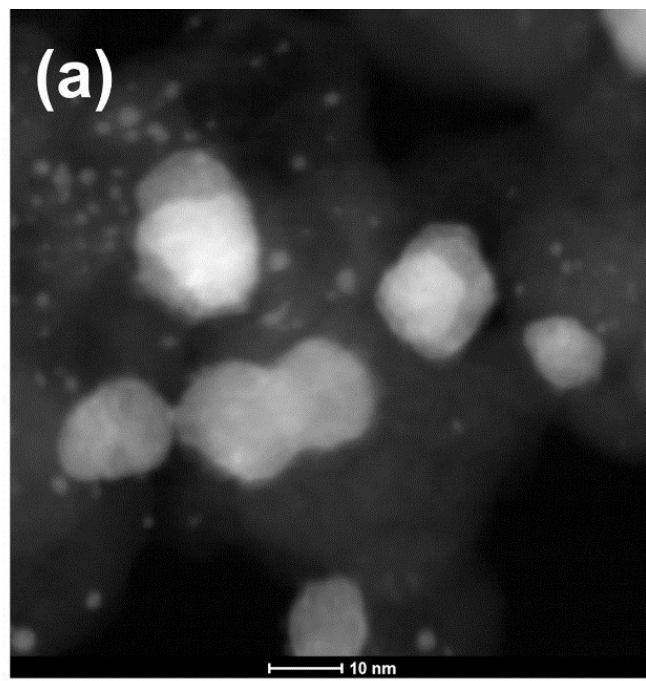


**Figure S2.** Identical location high angle annular dark-field STEM (IL-HADDF-STEM) images of IrNi/C (a) before and (b) after electrochemical activation in the acidic electrolyte conditions.

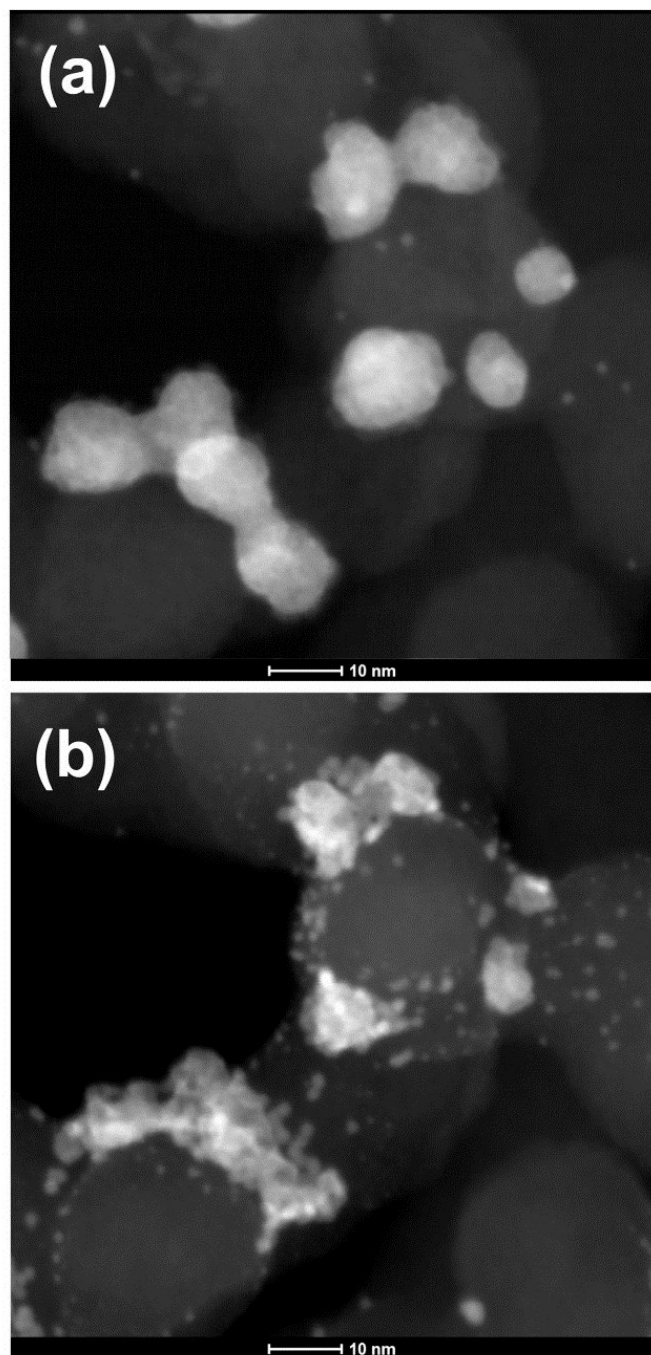


**Figure S3.** Identical location high angle annular dark-field STEM (IL-HADDF-STEM) images of IrNi/C (a) before and (b) after electrochemical activation in the neutral electrolyte conditions.

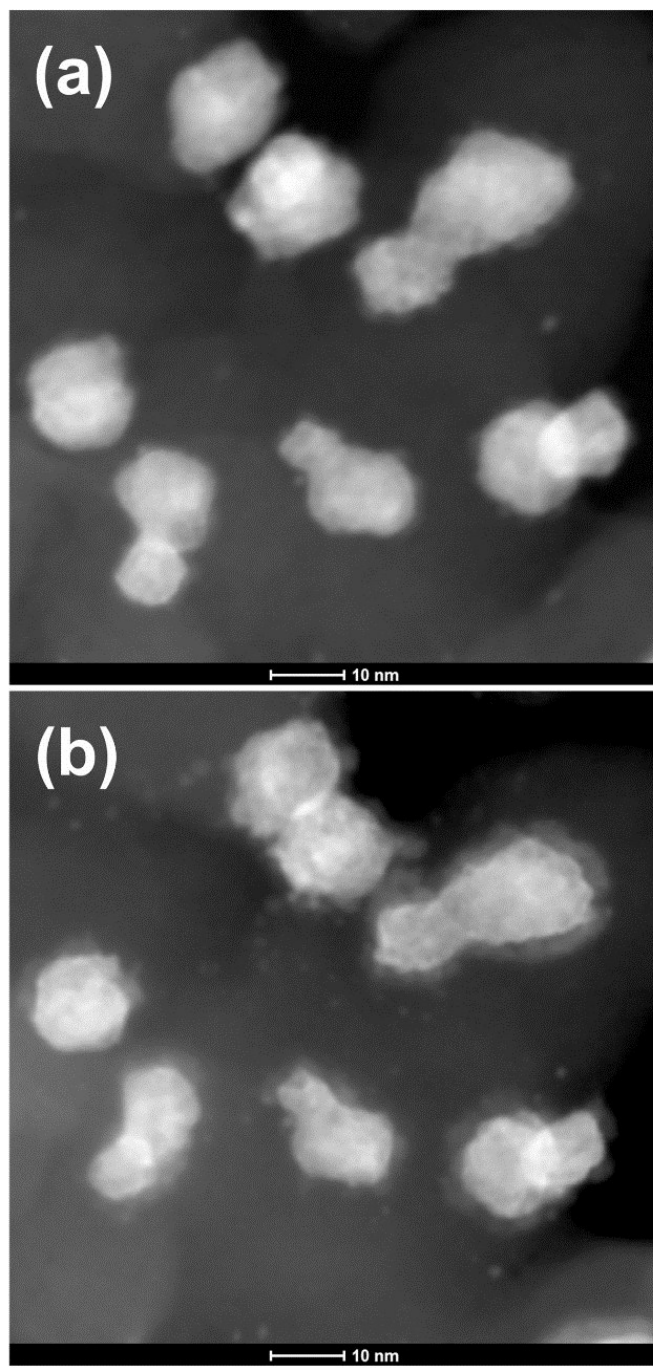


**Figure S4.** Identical location high angle annular dark-field STEM (IL-HADDF-STEM) images of IrNi/C (a) before and (b) after electrochemical activation in the alkaline electrolyte conditions.

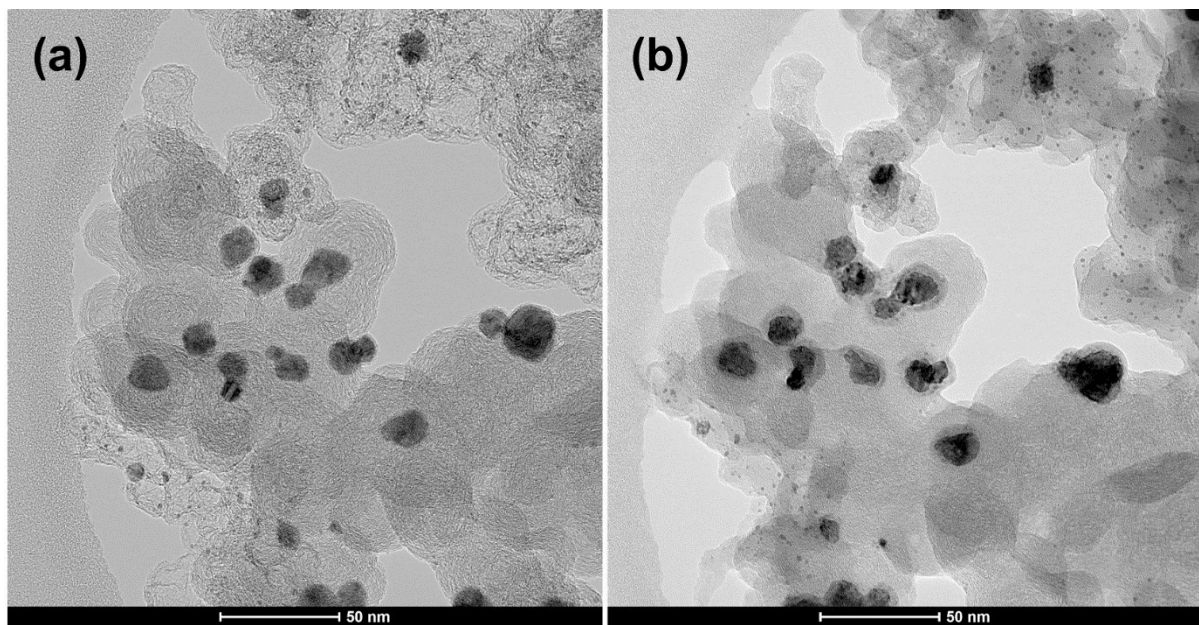


**Figure S5.** IL-TEM images of the IrNi/C (a) before and (b) after activation in the alkaline electrolyte conditions.

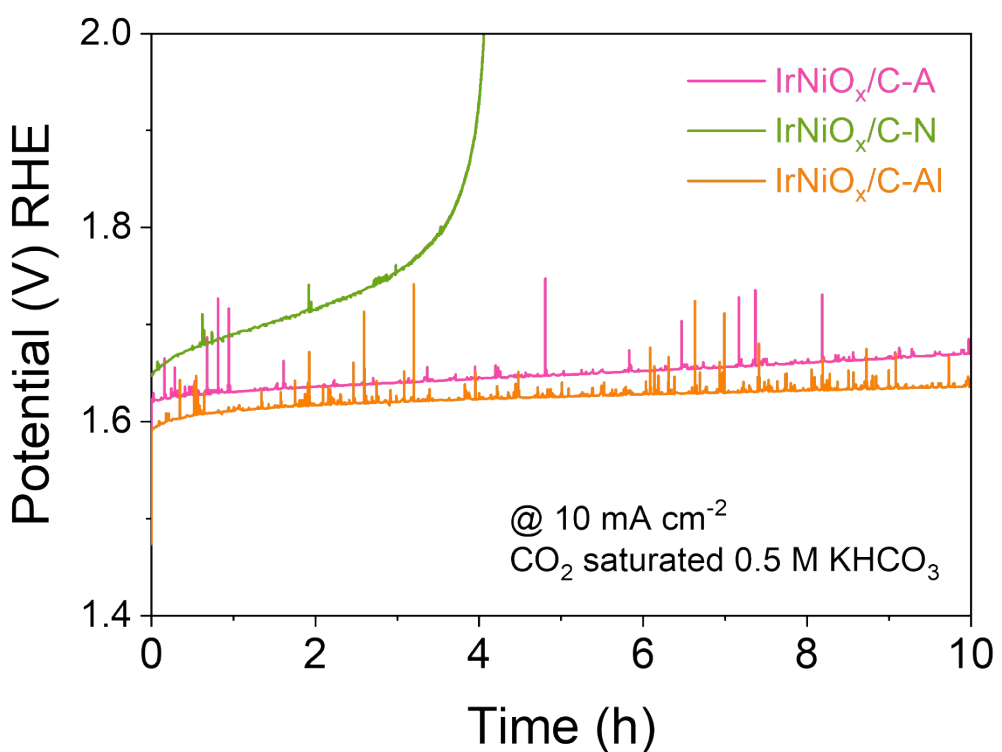


**Figure S6.** Constant current stability test of  $\text{IrNiO}_x$  based electrocatalysts for OER with different pH electrolyte activation conditions. Measurement condition: 25 °C, 10 mA cm<sup>-2</sup>, CO<sub>2</sub>-saturated 0.5 M KHCO<sub>3</sub>, 1600 rpm. Test time: 10 h. Ir loading: 20.5  $\mu\text{g cm}^{-2}$ .

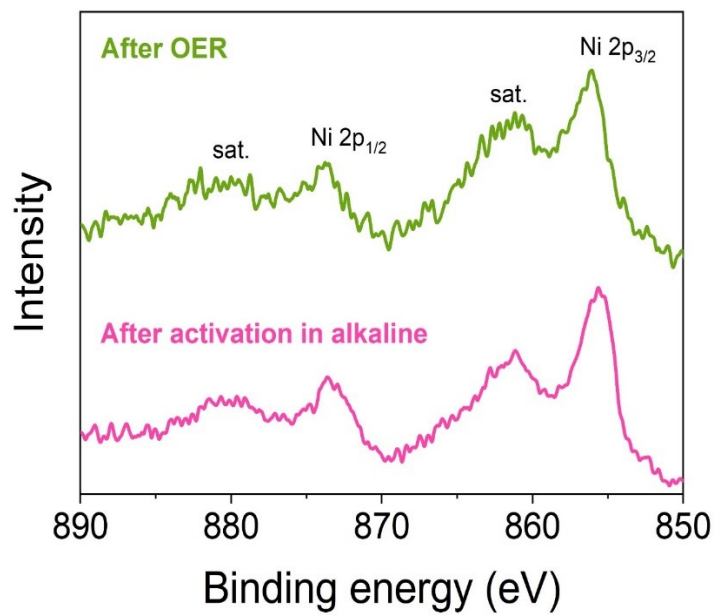


**Figure S7.** XPS spectra for Ni 2p of IrNiO<sub>x</sub>/C-Al (a) after electrochemical activation in alkaline condition and (b) after OER test in CO<sub>2</sub> saturated 0.5 M KHCO<sub>3</sub>.

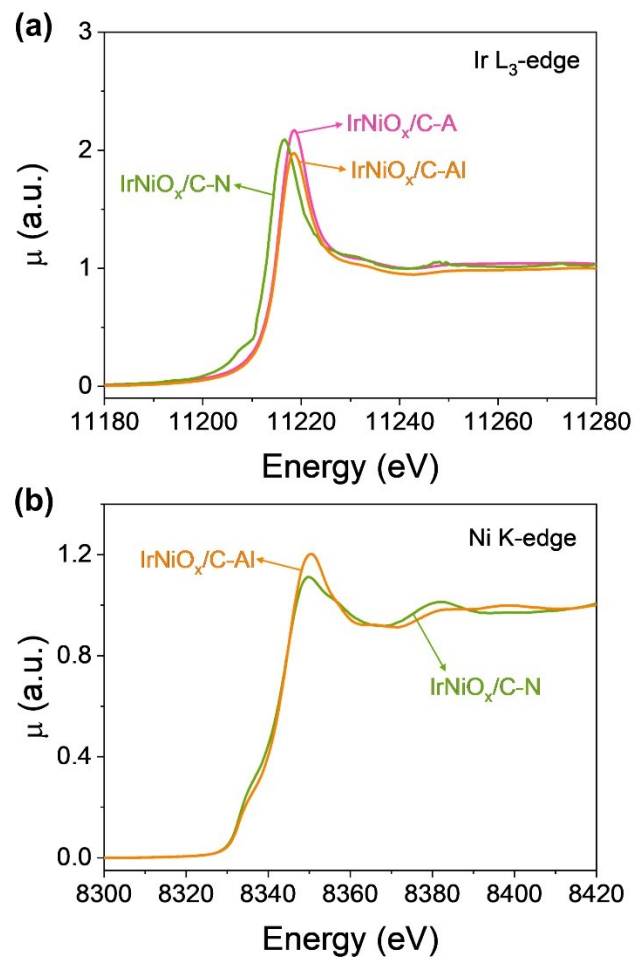


**Figure S8.** *Ex-situ* X-ray absorption spectroscopy (XAS) results of  $\text{IrNiO}_x/\text{C-A}$ ,  $\text{IrNiO}_x/\text{C-N}$ , and  $\text{IrNiO}_x/\text{C-Al}$ . NEXAFS region of (a) Ir L<sub>3</sub>-edge and (b) Ni K-edge.

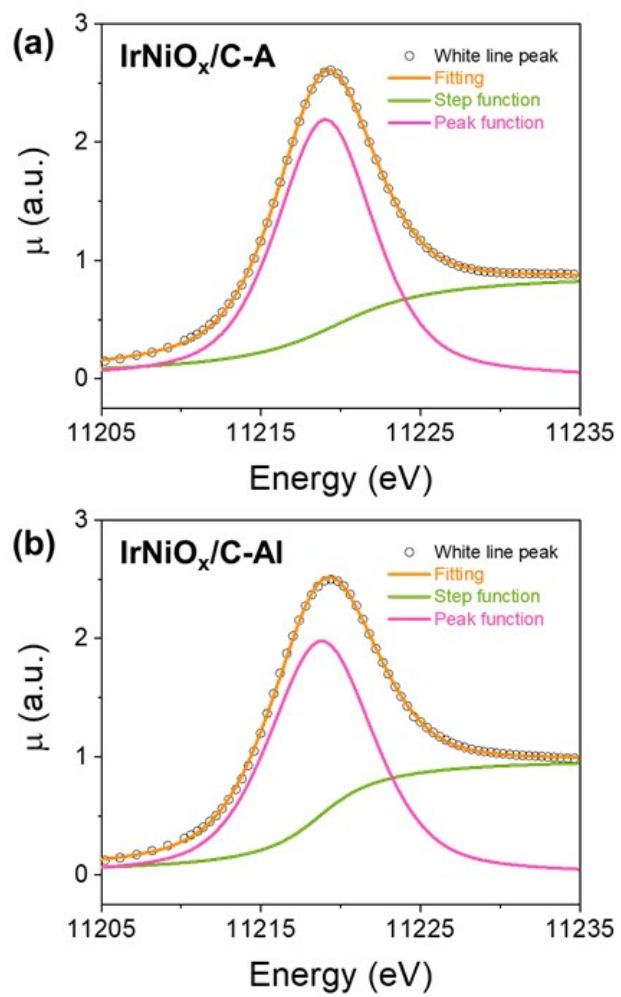


**Figure S9.** XANES Peak area fitting results of (a)  $\text{IrNiO}_x/\text{C-A}$  and (b)  $\text{IrNiO}_x/\text{C-Al}$ .

**Table S1.** Comparisons of OER electrocatalytic activity in neutral media

Catalyst	Catalyst loading (mg/cm <sup>2</sup> )	Tafel slope (mV/dec)	Potential (mV) @ 10mA/cm <sup>2</sup>	Reference
IrNiO <sub>x</sub> /C-Al	0.02	150	384	This work
Ni <sub>0.1</sub> Co <sub>0.9</sub> P	0.58	133	~530	Yu et al <sup>1</sup>
Co@Co-Bi/Ti	0.2	-	470	Wang et al <sup>2</sup>
Iridium incorporated Co(OH) <sub>2</sub>	0.566	117.5	373	Song et al <sup>3</sup>
Dendritic IrTe NTs	0.0245	77.9	570	Lin et al <sup>4</sup>
Ir <sub>70</sub> Ni <sub>15</sub> Co <sub>15</sub>	1.08	63.5	290	Tan et al <sup>5</sup>
IrRu@Te	0.15	-	309	Liu et al <sup>6</sup>
Li-IrSe <sub>2</sub>	0.25	-	315	Zeng et al <sup>7</sup>

## Reference

1. R. Wu, B. Xiao, Q. Gao, Y. R. Zheng, X. S. Zheng, J. F. Zhu, M. R. Gao and S. H. Yu, *Angewandte Chemie*, 2018, **130**, 15671-15675.
2. C. Xie, Y. Wang, D. Yan, L. Tao and S. Wang, *Nanoscale*, 2017, **9**, 16059-16065.
3. Y. Zhang, C. Wu, H. Jiang, Y. Lin, H. Liu, Q. He, S. Chen, T. Duan and L. Song, *Advanced Materials*, 2018, **30**, 1707522.
4. Q. Shi, C. Zhu, D. Du, J. Wang, H. Xia, M. H. Engelhard, S. Feng and Y. Lin, *Journal of Materials Chemistry A*, 2018, **6**, 8855-8859.
5. Y. Zhao, M. Luo, S. Chu, M. Peng, B. Liu, Q. Wu, P. Liu, F. M. F. de Groot and Y. Tan, *Nano Energy*, 2019, **59**, 146-153.
6. J. Xu, Z. Lian, B. Wei, Y. Li, O. Bondarchuk, N. Zhang, Z. Yu, A. Araujo, I. Amorim and Z. Wang, *ACS Catalysis*, 2020, **10**, 3571-3579.
7. T. Zheng, C. Shang, Z. He, X. Wang, C. Cao, H. Li, R. Si, B. Pan, S. Zhou and J. Zeng, *Angewandte Chemie*, 2019, **131**, 14906-14911.